Ocean Dynamics (2012) 62:265–281
DOI 10.1007/s10236-011-0497-1

Sensitivity of acoustic propagation to uncertainties in the marine environment as characterized by various rapid environmental assessment methods

Sean Pecknold · John C. Osler

Received: 1 March 2011 / Accepted: 19 September 2011 / Published online: 26 November 2011
© Her Majesty the Queen in Right of Canada 2011

Abstract Accurate sonar performance prediction modelling depends on a good knowledge of the local environment, including bathymetry, oceanography and seabed properties. The function of rapid environmental assessment (REA) is to obtain relevant environmental data in a tactically relevant time frame, with REA methods categorized by the nature and immediacy of their application, from historical databases through remotely sensed data to in situ acquisition. However, each REA approach is subject to its own set of uncertainties, which are in turn transferred to uncertainty in sonar performance prediction. An approach to quantify and manage this uncertainty has been developed through the definition of sensitivity metrics and Monte Carlo simulations of acoustic propagation using multiple realizations of the marine environment. This approach can be simplified by using a linearized two-point sensitivity measure based on the statistics of the environmental parameters used by acoustic propagation models. The statistical properties of the environmental parameters may be obtained from compilations of historical data, forecast conditions or in situ measurements. During a field trial off the coast of Nova Scotia, a set of environmental data, including oceanographic and geoacoustic parameters, were collected together with acoustic transmission loss data. At the same time, several numerical models to forecast the oceanographic conditions were run for the area, including 5- and 1-day forecasts as well as nowcasts. Data from the model runs are compared to each other and to in situ environmental sampling, and estimates of the environmental uncertainties are calculated. The forecast and in situ data are used with historical geoacoustic databases and geoacoustic parameters collected using REA techniques, respectively, to perform acoustic transmission loss predictions, which are then compared to measured transmission loss. The progression of uncertainties in the marine environment, within and between different REA categories, and the consequences on acoustic propagation are examined.

Keywords Rapid environmental assessment · Acoustic modelling · Propagation sensitivity

Responsible Editor: Michel Rixen

This article is part of the Topical Collection on *Maritime Rapid Environmental Assessment*

S. Pecknold (✉)
DRDC Atlantic, 9 Grove St., Dartmouth,
NS, Canada B2Y3Z7
e-mail: sean.pecknold@drdc-rddc.gc.ca

J. C. Osler
NATO Undersea Research Centre, Viale S. Bartolomeo
400, 19126 La Spezia, SP, Italy

1 Introduction

Rapid environmental assessment provides deployed forces with environmental information in littoral waters in tactically relevant time frames. The environmental data collected can come from historical sources, remote sensing tools, gliders and autonomous vehicles, or in situ assets.

NATO ExTac 777 separates REA into four categories (Whitehouse et al. 2006), based on the timeliness of data acquisition, also generally corresponding to ease or covertness of data acquisition. In the following discussion, category I REA is used to describe readily accessed, free environmental databases; category II REA refers to more detailed, pre-cursor data, acquired in advance of deployment of forces; category III REA, typically data obtained covertly, such as by gliders, was not acquired during the experiment upon which this paper is based and category IV REA refers to data collected in situ. Each REA category has uncertainties associated with it. That is, for each source of data, there is uncertainty associated with a lack of complete knowledge, for example, due to sparse sampling of bottom properties, or due to intrinsic variability of the oceanography. In order to have the best knowledge available for deployed sources, we require an understanding of the sources of these uncertainties and how they translate into impacts on sonar performance prediction and ultimately decision-making processes. Progression through REA categories can be expensive in resources and time. Therefore, it is important to know what to measure to most effectively use time and resources.

In this paper, we illustrate the use of REA data to categorize propagation uncertainty with a prototype tactical decision aid, the Portable Acoustic Sensitivity Transmission Evaluation Tool (PASTET; Giles et al. 2009), using environmental and acoustic data obtained during a sea trial. Environmental data corresponding to various REA categories were acquired. These are used to generate sensitivity analyses, or estimates of how environmental uncertainty translates into uncertainty in acoustic propagation. In particular, we wish to quantify the relative sensitivity of acoustic propagation to water and seabed parameters.

2 Uncertainty and acoustic propagation

The effect of oceanographic and geoacoustic uncertainty on acoustic propagation and sonar performance prediction has been of interest for a number of years and the subject of several conferences (Potter and Warn-Varnas 1990; Pace and Jensen 2002). The impacts of this uncertainty and variability have been studied in the context of various propagation models and experiments (Flatté et al. 1979; Krolik 1992; Finette 2006), and analytic computations of the sensitivity of propagation and reverberation in a waveguide on oceanographic and some geoacoustic (sound speed and attenuation, or complex sound speed) parameters have also been developed (LePage 2006). One method that may be used to compute sensitivity, described in Dosso et al. (2007), uses Monte Carlo sampling to draw random model parameter perturbations δm_j from a Gaussian distribution with mean m_j based on measured geoacoustic and oceanographic parameters. A forward propagation model is used to compute the corresponding model output p (in this case, the pressure field) for each sample. The sensitivity S_j is then the normalized RMS ensemble-averaged perturbation for each point of the pressure field relative to each model parameter:

$$S_j = \frac{\langle |p(m_j + \delta m_j) - p(m_j)|^2 \rangle^{1/2}}{|p|}. \quad (1)$$

This method can be used in environments with range-dependent bathymetry. An approximate linearized two-point sensitivity measure $\tilde{S}_j$ can also be defined using acoustic pressure p based on mean model parameters m_j with standard deviation σ_j (Dosso et al. 2007),

$$\tilde{S}_j = \frac{1}{2}\left(\frac{|p(m_j+\sigma_j) - p(m_j)|}{|p|} + \frac{|p(m_j-\sigma_j) - p(m_j)|}{|p|}\right). \quad (2)$$

The sensitivity calculations presented herein are undertaken using the PASTET. PASTET was developed to provide both transmission loss estimates (passive only in the prototype implementation), sensitivity measures as well as an envelope of expected transmission loss based on the mean and uncertainty of environmental parameters. The tool queries a REA database, which serves as a repository for ocean model forecasts, expendable bathythermograph (XBT) or other oceanographic profiles, as well as various existing environmental databases. The area of interest may be specified as a geographic area or by range along a bearing, and the bathymetric, oceanographic and geoacoustic data required for running an acoustic propagation model are returned. The propagation model used in the current PASTET system is the Bellhop Gaussian beam model (Porter and Bucker 1987). PASTET runs the Bellhop model using a range-dependent bathymetry, with range-independent sound speed profile and ocean bottom properties. The model has been modified to calculate bottom losses using a two fluid layer model, with Rayleigh reflection coefficients at each interface and volume attenuation. In the cases considered here, the sediment layer was assumed to be a half-space; therefore, the parameters required are compressional sound speed c_p, density ρ and attenuation α. PASTET is used to compute an incoherent transmission loss (TL). Surface loss is calculated using the Beckmann–Spezzichino model based on wind speed.

Given the expected use of PASTET as a tactical decision aid, the sensitivity calculations undertaken with it are made using the linearized sensitivity measure, which is expected in most cases to reasonably approximate the non-linear measure (Dosso et al. 2007). Uncertainty in the bottom properties is treated by assuming that the three surficial sediment parameters c_p, ρ and α are Gaussian and using the mean $\pm$ 1 standard deviation in the two-point sensitivity measure from Eq. 2. There are a number of ways in which uncertainty in the bathymetry can be treated. One way is to use the power spectrum of the roughness of the bottom to produce different roughness realizations (Rouseff and Ewart 1995), suitable for performing a full Monte Carlo sensitivity analysis. This will typically give large differences in coherent transmission loss due to the interference structure, but less so in the incoherent transmission loss case or possibly at long ranges (Thorsos et al. 2002), where the spatial variability may be smoothed by multiple interactions with the rough boundary. The effects of undersampling, or uncertainty at finer scales, have also been examined, showing TL errors that increase with coarsening bathymetry up to some frequency-dependent resolution (McCammon et al. 2007). In PASTET, the uncertainty in the bathymetry is treated by sampling a fan of bathymetric profiles along radials centred on the sensitivity run radial. The spacing is calculated such that the distance between the radials at their midpoint is matched to the grid size of the bathymetry source. Thus, the bathymetry samples are independent at the midpoint of the radials. The mean and standard deviation are then calculated on a point-by-point basis at each range step.

PASTET follows a similar procedure for oceanographic uncertainty using the linearized sensitivity measure, calculating the mean sound speed profile and the point-by-point standard deviations at each depth from a set of SSPs selected either along a track or from an area of ocean. Obviously a point-by-point sampling of sound speed is not appropriate for the Monte Carlo sampling, as this can result in non-physical sound speed profiles. In this case, most of the variance can be captured using the mean SSP, and the residual profiles can then be decomposed into empirical orthogonal functions (LeBlanc and Middleton 2006), with uncertainties characterized by the EOF eigenvalues. The same procedure can be followed for determining a set of perturbed bathymetries given the fan of bathymetric profiles used for determining the mean and standard deviations. In the following section, PASTET is used to produce transmission loss and linearized sensitivity estimates for several data sets; the sensitivity estimates produced are then compared to those computed using the Monte Carlo sampling technique corresponding to Eq. 1.

3 Experimental results

3.1 Field trial

In November 2009, a field trial, designated Q325, was undertaken in the area of Emerald Basin and Emerald Bank, on the Scotian Shelf. One-way transmission loss runs were conducted on November 3 and November 5. Two subsurface hydrophone acoustic recording packages (SHARPs), each with two hydrophones recording at 22.05 kHz, were deployed as moored receivers during each run. The first was deployed at 43°41.555′ N, 62°39.930′ W, in water of 148 m depth. The hydrophones were at depths of 52 and 72 m. The second SHARP was deployed at 43°50.823′ N, 62°51.161′ W, in 257 m of water. The hydrophones were again at 52 and 72 m depth.

On November 5, a source was deployed from CFAV Quest and towed at a speed of approximately five knots along the line between the two SHARP units. The source was towed at a depth that varied between 75 and 90 m and transmitted a series of CW tones and 200-Hz bandwidth LFMs at centre frequencies of 1,200 and 3,000 Hz. The waveforms were 10% Tukey weighted, with duration of 0.5 s, with 10 s inter-ping interval. Source level was approximately 190 dB re 1 μPa^2/Hz @ 1 m.

During the course of the transmission loss run, a mixed set of XBT, expendable sound velocity (XSV) and conductivity–temperature–depth (CTD) measurements were made. The surficial sediment type along the transmission loss line was characterized using a free-falling cone penetrometer (FFCPt) on November 4. The results from these environmental measurements will be discussed in Section 3.4.

3.2 Category I REA

An initial estimate of acoustic propagation sensitivity was made for the area of the experimental trial using category I REA data, consisting of readily available gridded databases for bathymetry, sediment type and oceanography. The analysis for this and other categories of REA data was performed for a frequency of 1,200 Hz, so as to match one of the transmit frequencies for the transmission loss experiment. The ETOPO2 gridded database (National Geophysical Data Center 2011) was used to obtain bathymetry data. Temperature and salinity profiles were obtained from monthly climatology from the World Ocean Atlas (Antonov et al. 2006; Locarnini et al. 2006) in the experimental area and converted to sound speed profiles using del Grosso's equation (Del Grosso 1970) with

Table 1 Geoacoustic parameters for category I REA

	Mean	σ
c_p (m/s)	1,645	166
ρ (g/cm^3)	1.64	0.44
α (dB/m-kHz)	0.60	0.36

modifications (Wong and Zhu 1995) where applicable (Chen and Millero algorithm (Chen et al. 1977) outside the range of applicability). Geoacoustic information was obtained from the DECK41 sediment database (Bershad and Weiss 1975). The sediment names found in the database were translated to grain size (Jackson 1994), thence to compressional sound speed c_p, density ρ and attenuation α. The mean and standard deviation for these parameters for data in the experimental area are given in Table 1. For this and the other REA categories, sediment thickness is neglected. It is unavailable in this database, but in general the sediment is quite thick in the Emerald Basin area (on the order of tens of metres), and the sensitivities to the first layer are typically orders of magnitude higher than to the basement at these frequencies in this area.

Linearized sensitivity calculations were performed for the category I REA environmental data using Eq. 2, with the results from these calculations, along with the transmission loss field for the mean parameters, shown in Fig. 1. The transmission loss field is shown in decibels of transmission loss. The sensitivity results are shown as the sensitivity measure (relative changes in the acoustic pressure field based on expected uncertainty in model parameter) with respect to range and depth, in this case for a source at a depth of 52 m. The mean SSP is shown in the upper left-hand part of Fig. 1, while the mean and perturbed SSPs are shown as solid and

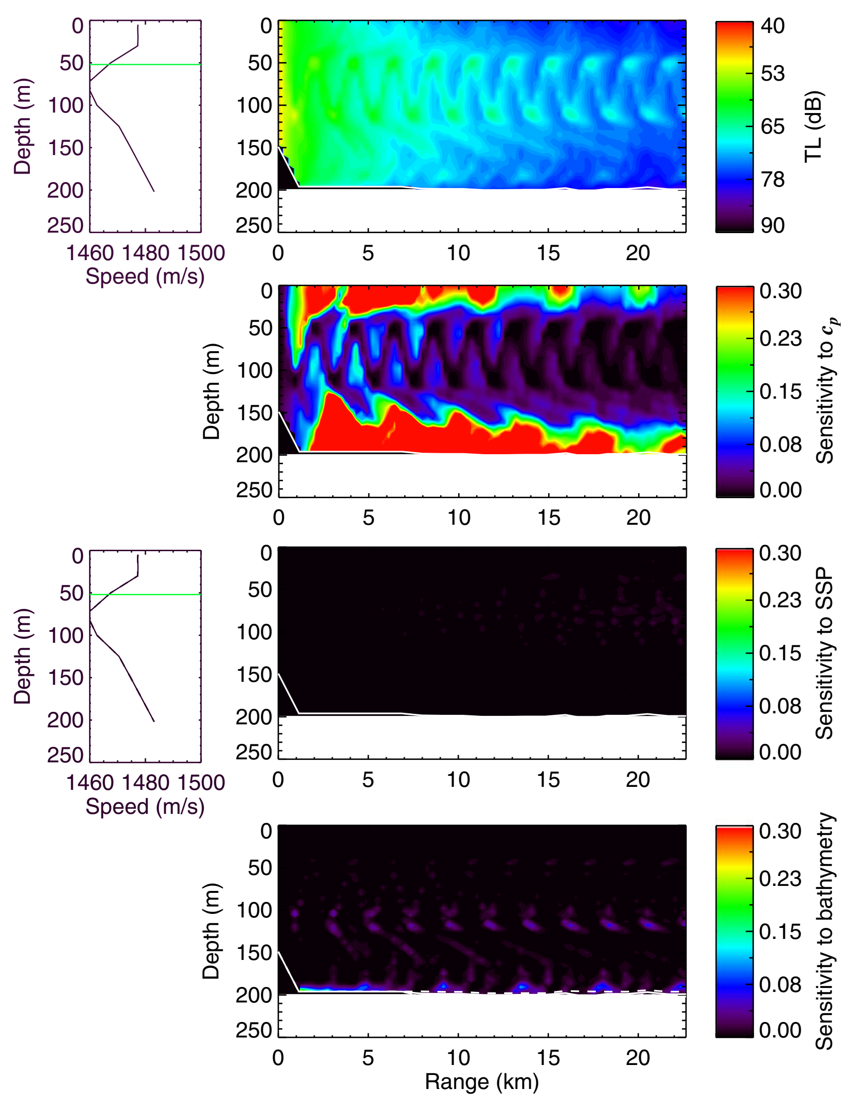

Fig. 1 REA category I transmission loss and sensitivity fields for c_p, SSP and bathymetry

dashed lines, respectively, in the third row of the left-hand column of the figure. These were derived from a total of 24 profiles obtained from monthly climatology in a box around the experimental area. Due to the lack of variability in the oceanographic database for the experimental area, the perturbed SSPs in this case are indistinguishable from the mean SSP in the figure, although there are very slight differences. The green line in the SSP plots indicates the assumed source depth, here 52 m. Mean and standard deviations for the geoacoustic parameters used in Eq. 2 are given in Table 1. Only the sensitivity of propagation to the compressional sound speed is shown in the sensitivity field figures, as the overall pattern for sensitivity to attenuation and sediment density is in general both similar to and less than that for c_{p}, as shown by example in Fig. 2. Sensitivity to uncertainty in the bathymetry was calculated using the method described in Section 2. It should be noted that the ETOPO2 bathymetry along the transmission loss run was erroneous. The mean bathymetry and expected uncertainty in it (outlying values used in the two-point linearized sensitivity calculation) are shown as solid and dotted lines, respectively, in the sensitivity field plot for the bathymetry (these are more evident in Fig. 4). The transmission loss shown in Fig. 1 is based on the mean input parameters and indicates that the acoustic energy is trapped in the mid-water column duct. The sensitivity of propagation to the various environmental parameters changes with respect to both range and depth, in particular to the geoacoustic properties of the surficial sediment. As an example, given a target at the depth of 52 m as simulated here, the performance of a hull-mounted sonar would depend far more on the bottom parameters than would a towed array, particularly at shorter ranges. To a degree, this is also driven by the large uncertainties on knowledge of the sediment properties.

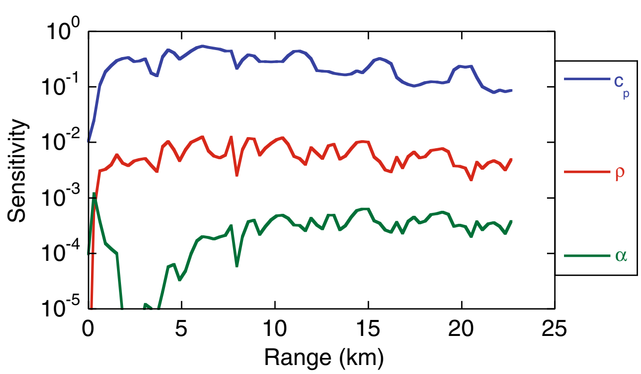

Fig. 2 Comparison of sensitivity measures for c_{p}, ρ and α for category I environmental data vs. range at a receiver depth of 4 m. Source is at 52 m depth

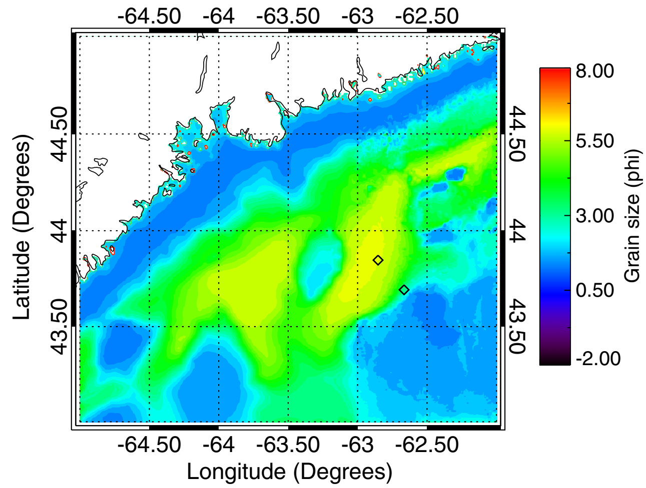

Fig. 3 Surficial sediment grain size. SHARP locations shown as *diamonds*

In this example, sensitivity to both the SSP and bathymetry is (artificially) low, due to a lack of sufficient variability in the databases to obtain meaningful statistics on our uncertainty. Because the sensitivity measure is based on the propagation sensitivity to 'typical' variability or uncertainty in the oceanography, the low sensitivity to SSP found here is an artifact of the spurious certainty obtained from the category I data. In addition, the sensitivity to bathymetric uncertainty here shows evidence of the field shifting effects of environmental perturbation (Dosso et al. 2007). Specifically, sensitivity will be high near the boundaries of the long-range propagation path, indicating that the acoustic path has shifted slightly in space due to the environmental perturbation.

Given that we have insufficient statistics to develop meaningful sensitivities to the water column, we can extend the geographical area over which profiles are taken to include other water masses. This allows an estimate of uncertainty on SSP but can lead to physically unrealistic profiles, requiring a different procedure such as clustering the differing SSPs and examining the inter-cluster sensitivity changes. The change in behaviour of the TL field and on the sensitivity to the seabed indicates that the parameters all interact, and

Table 2 Geoacoustic parameters for category II REA

	Mean	σ
c_{p} (m/s)	1,499	30
ρ (g/cm^3)	1.17	0.03
α (dB/m-kHz)	0.33	0.22

therefore, some environmental knowledge is always required to obtain meaningful results. In this example, then, it is difficult to make a good estimate of sensitivity based on category I REA data.

3.3 Category II REA

Category II REA data are typically categorized as precursor data. For the purposes of this analysis, we will use a higher-resolution bathymetric data set, collected by the Canadian Hydrographic Survey (CHS), which gives gridded depth values with a spacing of approximately 500 m; an empirical model of sediment grain size based on the bathymetry and known properties of the Scotian Shelf and sound speed profiles from ocean forecasting models. The surficial sediment type on the Scotian Shelf is well-correlated with the water depth, due to historical sea level changes and transport of silt and clay from shallower areas to the deeper basins. Expressions for the grain size fraction for gravel $P_g(h)$, sand $P_s(h)$ and mud $P_m(h)$ as a function of water depth h on the Scotian Shelf have been developed (Furlong et al. 2006). A mean grain size $M_z(h)$ can then be defined in units of ϕ, i.e. $-10\log_2$ (grain size in millimetres),

$$M_z(h) = -0.5 P_g(h) + 2 P_s(h) + 7.9 P_m(h). \quad (3)$$

Given this mean grain size (shown in and around the experimental area in Fig. 3), formulae from the APL-UW Environmental Handbook (Jackson 1994) can then be used to calculate c_p, α and ρ. The mean and standard deviation for these parameters along

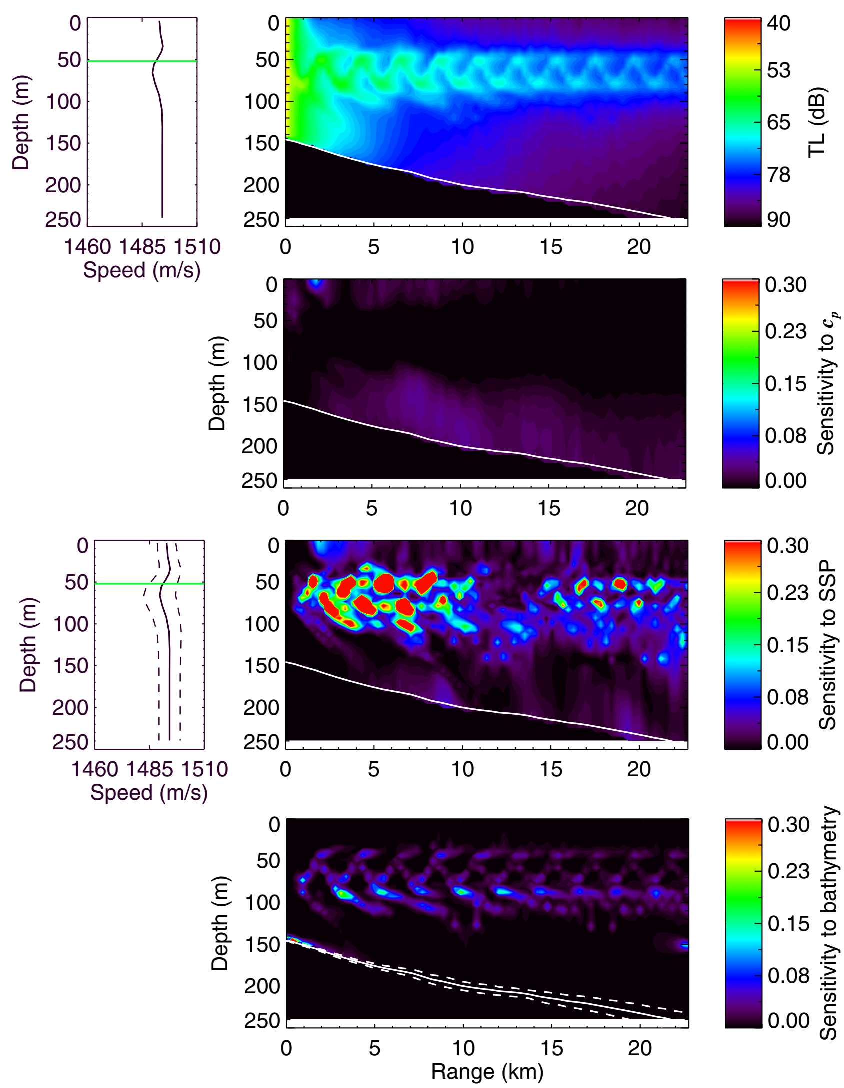

Fig. 4 REA category II transmission loss and sensitivity fields for c_p, SSP using the C-NOOFS model and CHS bathymetry

the transmission loss line were computed relative to a sound speed of 1,500 m/s in the water and are given in Table 2. It is evident that this method shows much softer sediment than tabulated in the DECK41 database.

During the course of the Q325 sea trial, SSP forecasts and nowcasts were available from several different ocean models. Sensitivity analyses were done using 1-day forecasts for 5 November 2009, using two models. These were Canada-Newfoundland Operational Ocean Forecasting System (C-NOOFS), a model run by the Department of Fisheries and Oceans that uses the Nucleus for European Modelling of the Ocean numerical model (Madec 2006) and the Global Navy Coastal Ocean Model (NCOM) (Rhodes et al. 2002). Both models produce 3D fields of temperature and salinity, with 50 vertical levels, C-NOOFS on a 1/12° grid and NCOM on a 1/8° grid. The models differ in their spatial resolutions, assimilation capabilities and wind and tidal forcings. Profiles in a 1/2° box around the experimental area were used to compute mean and perturbed SSPs for the sensitivity calculations. The mean and perturbed SSPs for the C-NOOFS model and NCOM are shown together with the transmission loss and sensitivity fields calculated using the CHS bathymetry and empirical grain size model, in Figs. 4 and 5. The solid lines in the SSP plots indicate the mean SSP, and the dashed lines in the third row indicate the perturbed SSPs. The green line in the SSP plots indicates the assumed source depth, again 52 m.

The sensitivity measures calculated using the two model forecasts are quite different. In both cases, there is significant sensitivity to the sound speed profile in the middle of the water column where the actual acoustic

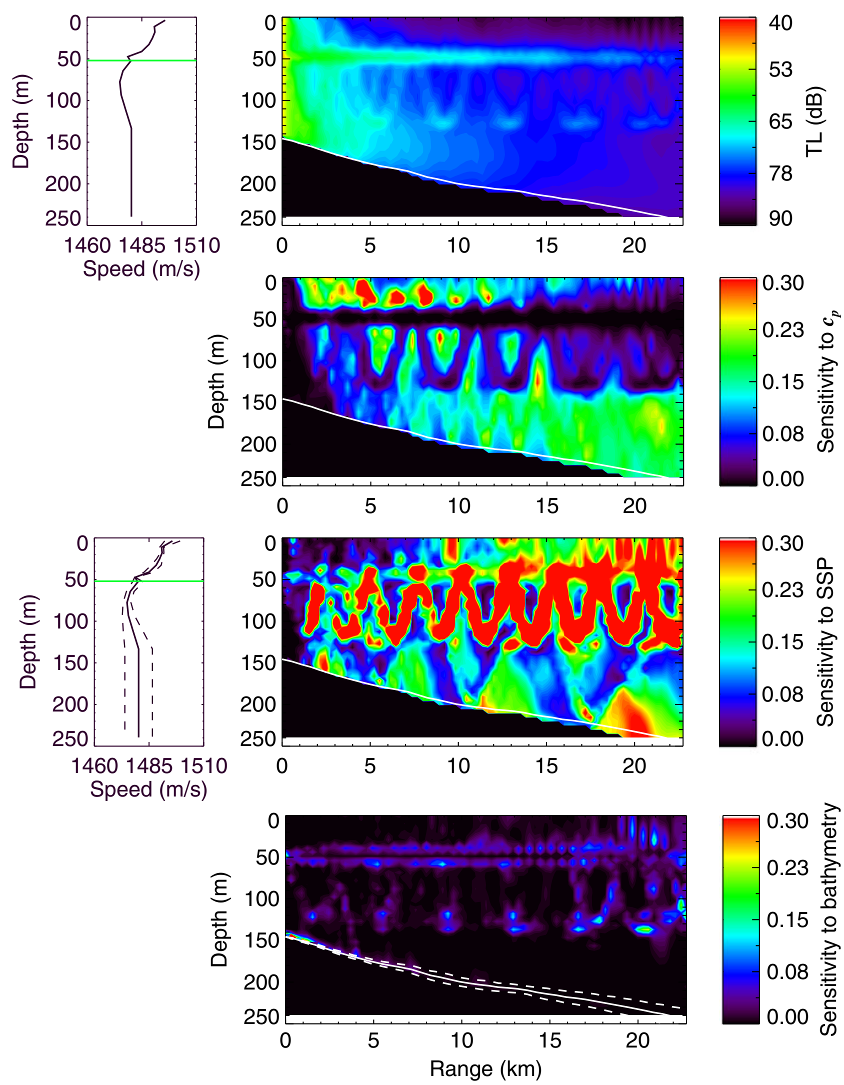

Fig. 5 REA category II transmission loss and sensitivity fields for c_p, SSP using the NCOM model and CHS bathymetry

energy is the highest. The sensitivity diminishes at increasing range in the C-NOOFS case but increases for the NCOM. The NCOM calculation also shows much higher sensitivity to the sea bottom, as one of the perturbed SSPs loses the mid-column duct. Although the variance of the geoacoustic parameters is lower than that found using category I REA, the sensitivity on these parameters is still significant. Much of the difference between the two sets of results seems to be due to the differing SSPs generated by the two model forecasts. For both models, most of the profiles show a fairly strong mid-column duct, characteristic of the Emerald Basin region at this time of year. However, the NCOM model generates another type of profile in the region as well, which is primarily downward refracting but with a sharp duct nearer the surface, giving a mean SSP that has a strong propagation path at this depth and significant variance through the lower part of the water column. The C-NOOFS model, on the other hand, seems to include water masses with different characteristics on the shallower part of the propagation path near the Emerald Bank, as it shows some isovelocity profiles that weaken the ducting, but do not create the potential downward refracting profile seen in the NCOM model.

There exists the issue of how best to estimate the true propagation sensitivity to the SSP in this case. Here we have effectively clustered the SSPs from individual models to gain an overall estimate of mean and perturbed propagation, as it is not clear that the mean of the two sets of model forecasts would be representative of the actual SSPs. As an alternative, a sensitivity analysis could be performed using sampling of the set of SSPs generated by an ensemble of models.

3.4 Category IV REA

Category IV REA data are that which could be collected by or with deployed forces. This can include bathymetry from single or multi-beam systems onscene, sound speed profiles measured using a moving vessel profiler and XBTs, and geoacoustic parameters and sediment thickness measured in situ using a FFCPt and sub-bottom profiler. During sea trial Q325, a series of 31 FFCPt drops was performed along the transmission loss line between the two SHARP units. The FFCPt gives acceleration and pore pressure data that can be used to obtain a sediment type (Osler et al. 2006), shown in Fig. 6 (bottom) as the Robertson zone (Robertson 1991). The FFCPt only samples the upper part of the sediment; in the analysis here, it is assumed that the bottom is a fluid half-space. As shown in the figure, the sediment becomes softer, with deeper penetration depths, as one moves from the shallower Emerald Bank into Emerald Basin and the sediment type changes from sand (zone 6) to silt (zone 5) and silty clay (zone 4). Similarly to the procedures for the previous categories of REA data, these sediment types can then be translated to grain size and geoacoustic parameters. Table 3 shows the mean and standard deviations for c_p, α and ρ for the FFCPt drops. Although these are consistent with the values found using the category II empirical formula, the overall impression is that Eq. 3 may underestimate the sediment variability.

Figure 6 (top) also shows the SSPs measured during the November 5 transmission loss run. During this run, a set of 13 XBT measurements of water column temperature profile were taken. CTD casts at the beginning and end of the run and an XSV cast in the middle of the run were also made, and these were used to obtain salinity profiles to compute the sound speed profiles from the XBT measurements.

As with the previous categories of REA data, a sensitivity analysis is done using the category IV data. The

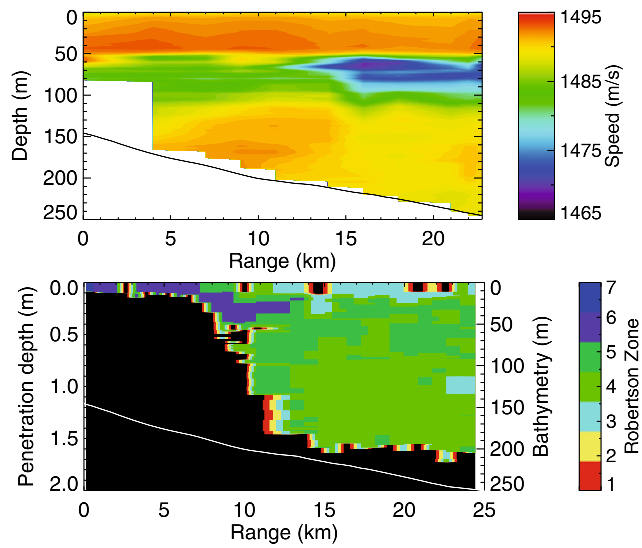

Fig. 6 Category IV REA environmental data: measured SSPs for 5 November (*top*) and sediment type by Robertson zone and bathymetry (*white line*) (*bottom*)

Table 3 Geoacoustic parameters for category IV REA

	Mean	σ
c_p (m/s)	1,586	154
ρ (g/cm^3)	1.42	0.40
α (dB/m-kHz)	0.34	0.23

results are shown in Fig. 7 for a 52-m deep source and Fig. 8 for a 72-m deep source. Sensitivity to the bottom is quite high for the 52-m source. In general, sensitivity to the bottom is fairly low in the sound channel for the 72-m depth, but higher near the boundaries, although the sensitivity decreases near the boundaries with increasing range. Sensitivity to bathymetry and sound speed profile shows evidence of the field shifting effects of environmental perturbation. Specifically, sensitivity will be high near the boundaries of the long-range propagation path, indicating that the path has shifted slightly in space due to the environmental perturbation. The impact of the environmental uncertainty will depend on the particular scenario. For example, for mid-water column propagation, general knowledge of the bottom with more knowledge of the oceanography should suffice; near the surface and bottom, a range-dependent bottom may be required, again with only a few measurements of SSP.

3.5 Comparison of linearized and non-linear sensitivities

PASTET uses the linearized (two-point) sensitivity measure under the assumption that it is a reasonable approximation to the full non-linear measure obtained by a Monte Carlo procedure. These can now be compared to the non-linear sensitivity fields. For each environmental parameter, 100 realizations were generated and propagated through the forward model, and the full-field sensitivity was generated. The EOFs used to generate the perturbed sound speed and bathymetric

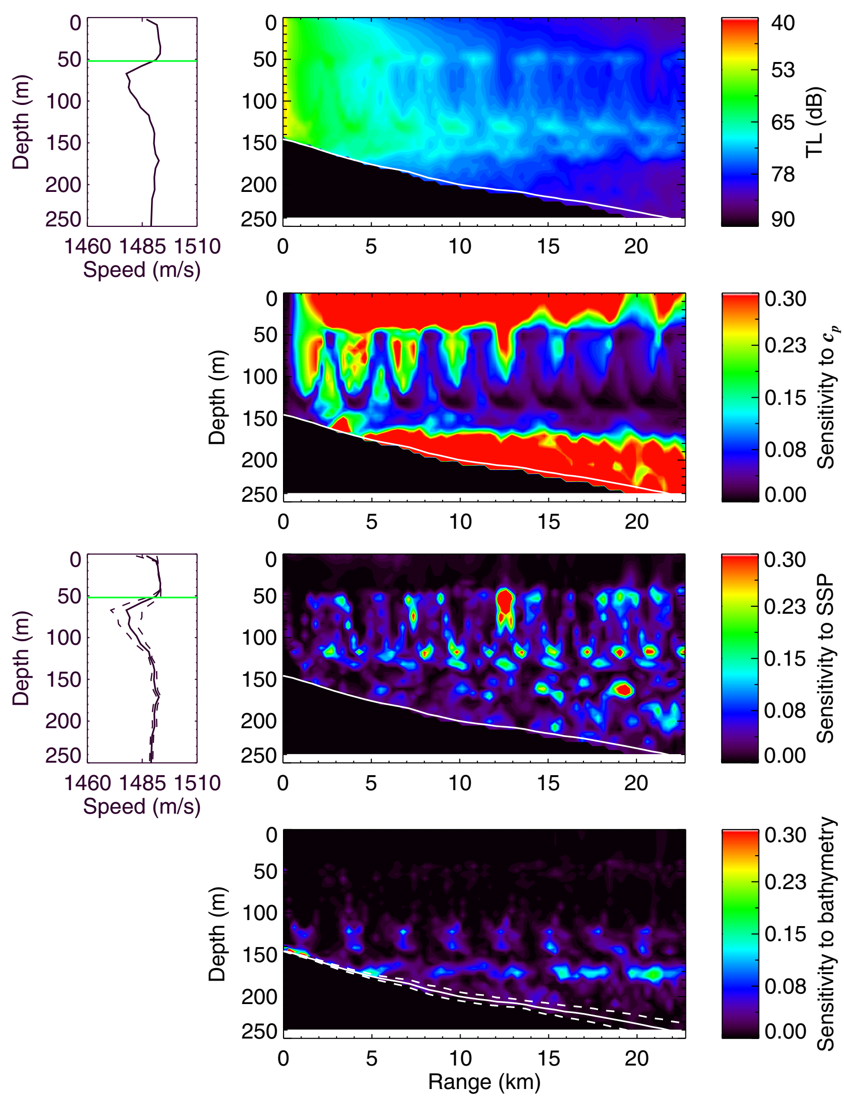

Fig. 7 REA category IV transmission loss and sensitivity fields for c_p, SSP and bathymetry. Source at 52 m depth

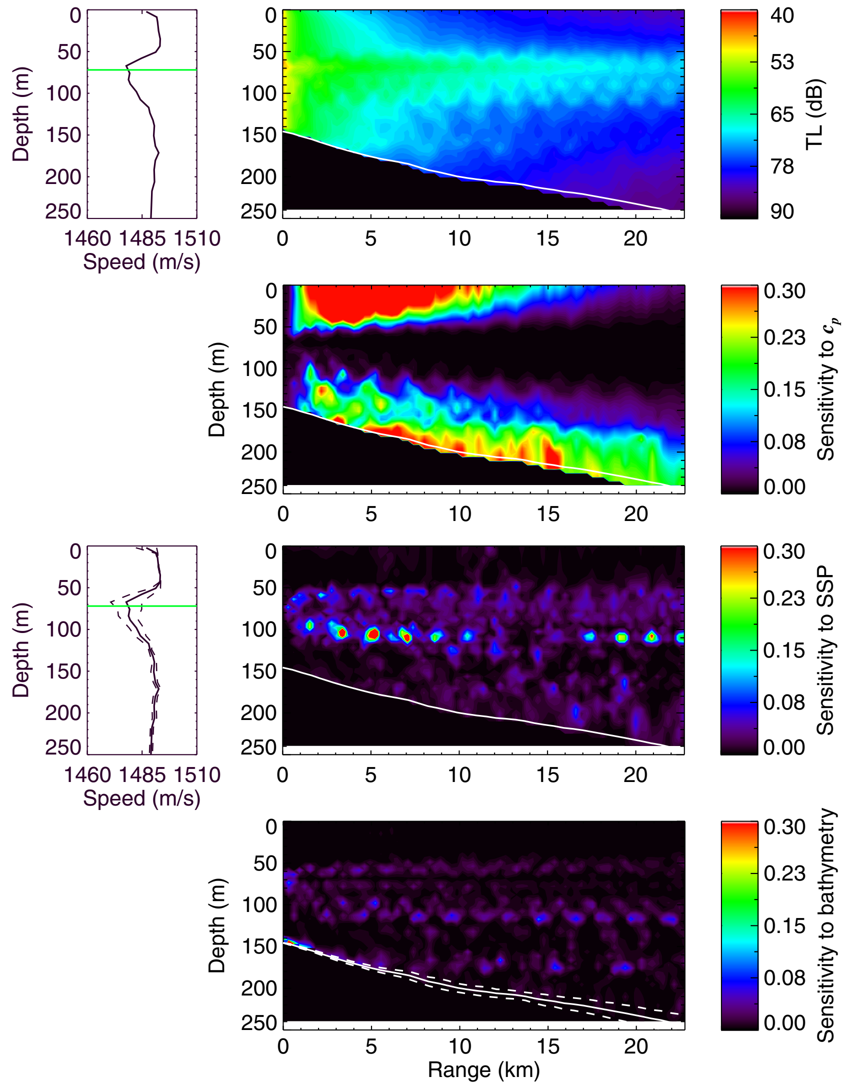

Fig. 8 REA category IV transmission loss and sensitivity fields for c_p, SSP and bathymetry. Source at 72 m depth

profiles include at least 97% of the variance of the data sets. As was the case with the linearized sensitivities, the effects of attenuation and density in the seabed are similar to but significantly less than that of the compressional sound speed; therefore, the results for these parameters are not shown. A comparison of the full-field results for c_p is shown in Fig. 9 and a comparison for sound speed profiles in Fig. 10. The scale range has been increased for the non-linear sensitivity results to facilitate comparison of the sensitivity field structure. It is possible that using only 100 realizations for computing the non-linear sensitivity might affect the results obtained. This was tested by generating a set of 500 realizations for the 52-m source for the category IV data. The sensitivities found for the bathymetry and bottom properties using the larger set were very similar in structure and value to those found using the smaller set of realizations, while the sensitivity to SSP was also very similar in structure, but with values averaging about 6% higher.

It is evident from Figs. 9 and 10 and considering that the scale has been increased for the non-linear sensitivity figures that the linearized sensitivity measure in general underestimates the sensitivity of the acoustic pressure field to typical environmental changes. Nevertheless, given the re-scaling of the fields, the range–depth behaviour of the sensitivity for the non-linear measure is quite similar to that of the linearized measure, with several exceptions. For the sensitivity to changes in the sound speed profile in particular, the non-linear measure spreads out the field more, with higher sensitivities than for the linearized case outside

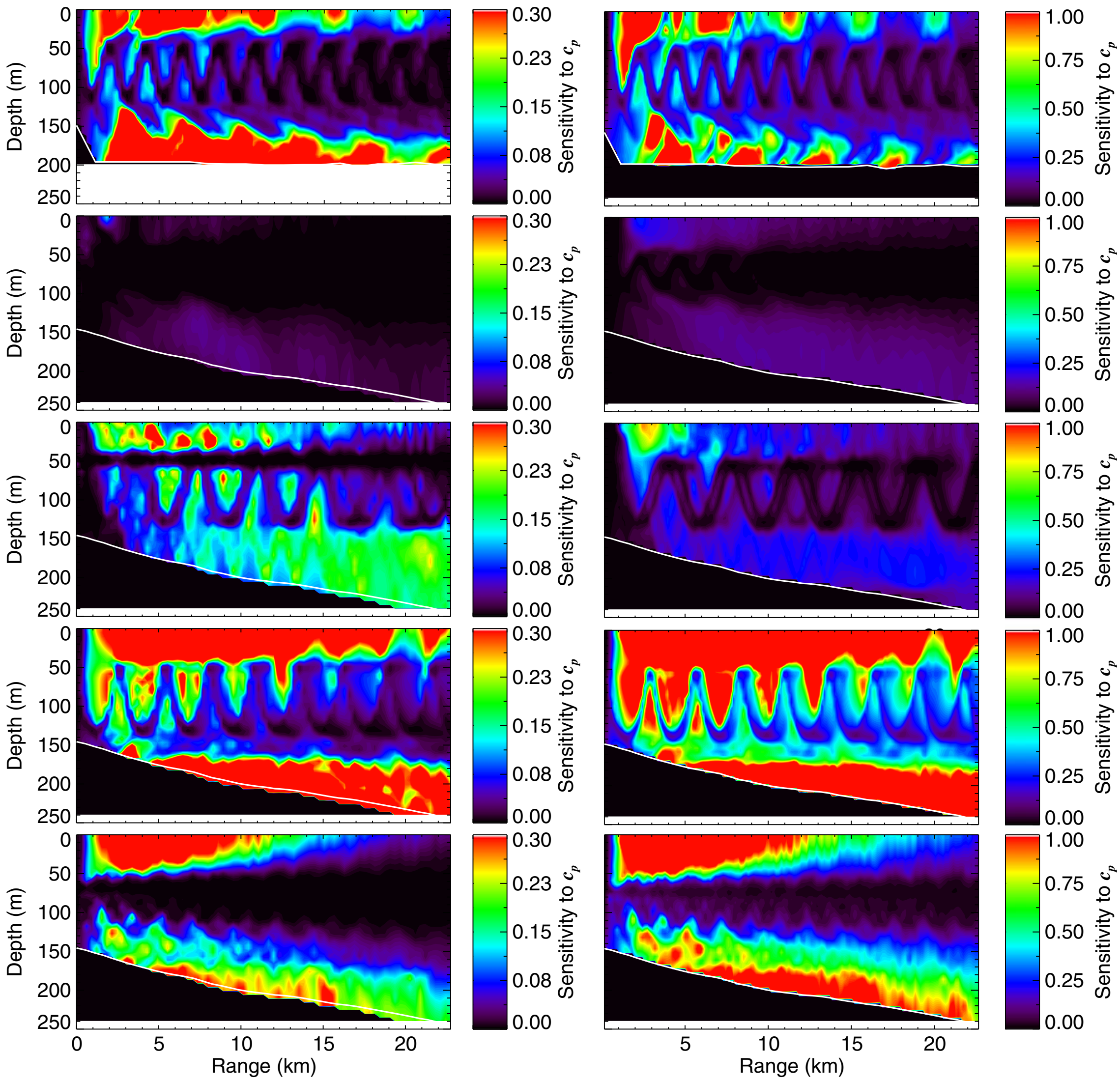

Fig. 9 Comparison of linearized sensitivity (*left column*) to non-linear sensitivity (*right column*) for c_p: REA category I data (*row 1*); REA category II, C-NOOFS (*row 2*); REA category II, NCOM (*row 3*); REA category IV (*rows 4* and *5*). Source at 52 m depth for *rows 1–4*, 72 m depth for *row 5*. Note that scale differs between *left and right columns*

the main sound channel. The other main exception is for both c_p and SSP in the case of the NCOM model data. The sensitivity to c_p shows a fairly similar structure to that for the linearized measure, but with fewer hot spots, and a greater sensitivity near the surface at short ranges. The difference between the general levels between the linearized and non-linear cases is also less for this environment than for the others. The sensitivity to the NCOM SSP data from Fig. 10 shows quite a large difference between the linearized and non-linear data, with much more variation in the behaviour within the sound channel seen in the non-linear measure.

To consider the question of the relative importance of each parameter in determining the overall sensitivity and how this differs between the two sensitivity measures, the sensitivity fields are averaged across several regions. Figure 11 shows the linearized and non-linear sensitivity measures averaged over range and depth for three sets of depths (surface from 0 to 20 m depth, sound channel or mid-column from 50 to 70 m depth and deep from 130 to 150 m depth). In this figure, the parameters within each category are ordered along the *x*-axis by first their environment, then by their magnitude in the mid-channel linearized sensitivity field. It

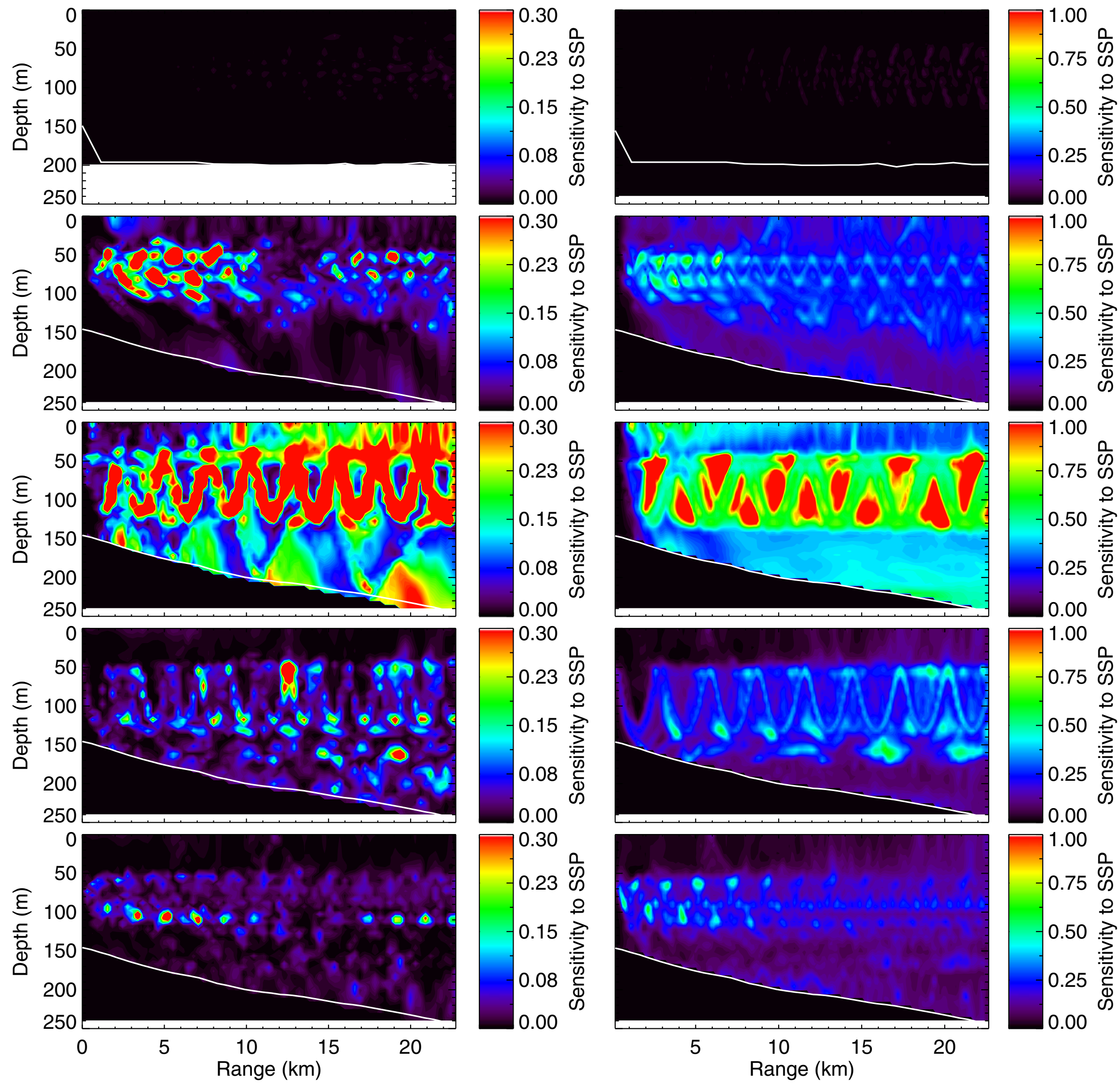

Fig. 10 Comparison of linearized sensitivity (*left column*) to non-linear sensitivity (*right column*) for SSP: REA category I data (*row 1*); REA category II, C-NOOFS (*row 2*); REA category II, NCOM (*row 3*); REA category IV (*rows 4* and *5*). Source at 52 m depth for *rows 1–4*, 72 m depth for *row 5*. Note that scale differs between *left and right columns*

is evident that in most cases, the non-linear sensitivity is higher by a considerable margin than the linearized sensitivity, although typically by less than an order of magnitude and less for the more important parameters than for the less important ones. In all cases except those of the deep water REA category II environment using the C-NOOFS data and the shallow water category II environment with NCOM, the most important parameter is the same for both the linearized and non-linear measure. In both these cases, sensitivity to the SSP and c_p, while inverted, is still quite similar to the other. For the category I environment, both the shallow and mid-channel depths invert the importance of the bathymetry and SSP; however, the sensitivity to either is at least 2 orders of magnitude less than that to c_p. The one major difference is for the 72-m source in the category IV environment, where the non-linear measure indicates that sediment properties are nearly as important as the SSP in the middle of the water column.

3.6 Transmission loss

The preceding sensitivity analyses were performed at a frequency of 1,200 Hz to facilitate comparison to the

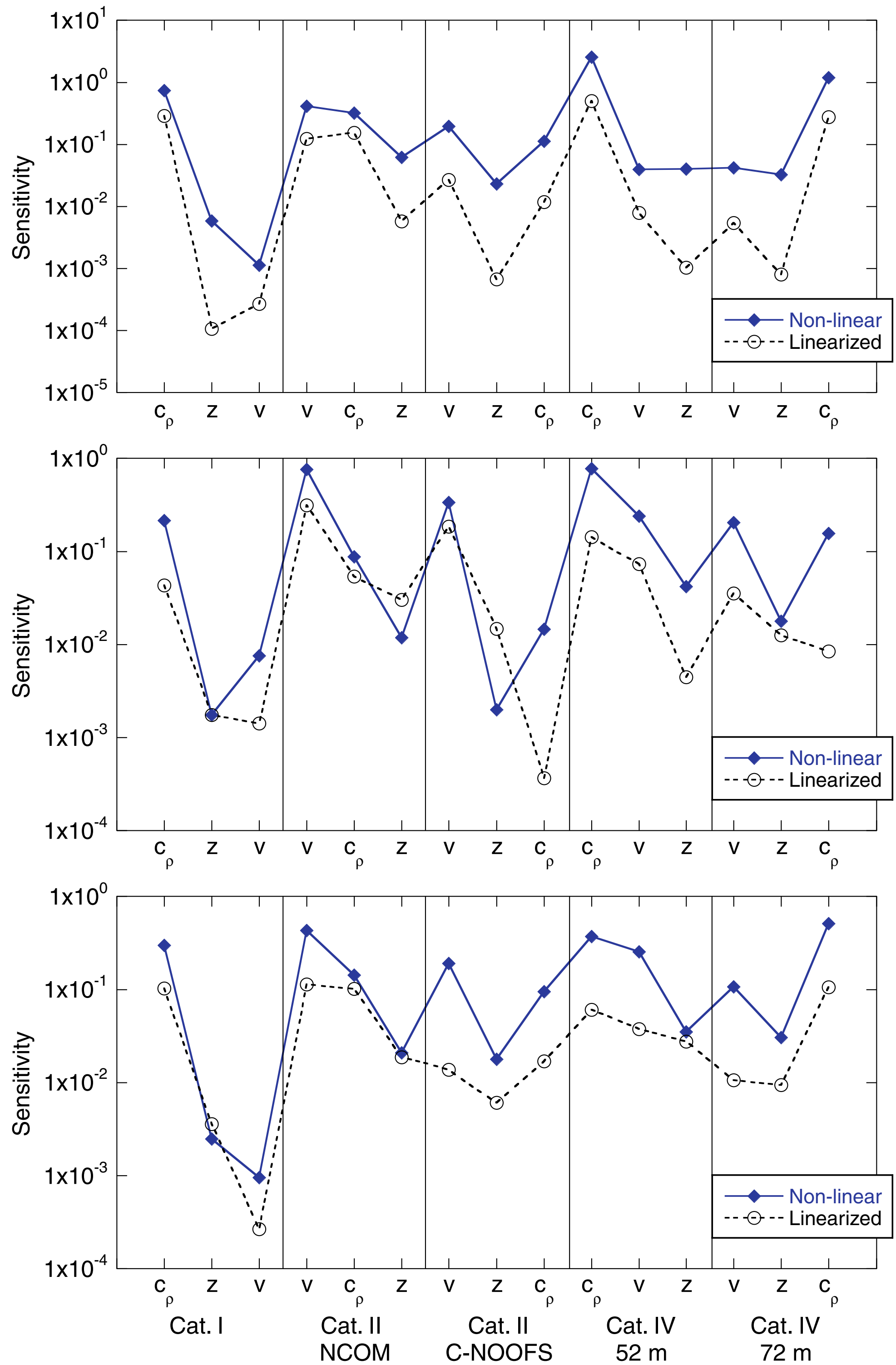

Fig. 11 Sensitivity measure averaged over 0–20-km range for five environments vs. parameter, where z indicates bathymetry, c_p indicates compressional sound speed in the sediment and v indicates sound speed profile. Averaged over 0–20 m depth (*top*), 50–70 m depth (*middle*), 130–150 m depth (*bottom*)

data measured during the Q325 sea trial. In addition to range- and depth-dependent fields showing how the propagation depends on the various environmental parameters, the transmission loss based on the mean environment and the transmission loss envelope generated by the perturbations in the model parameters were computed using the PASTET system. Figure 12 compares the incoherent transmission loss measured on

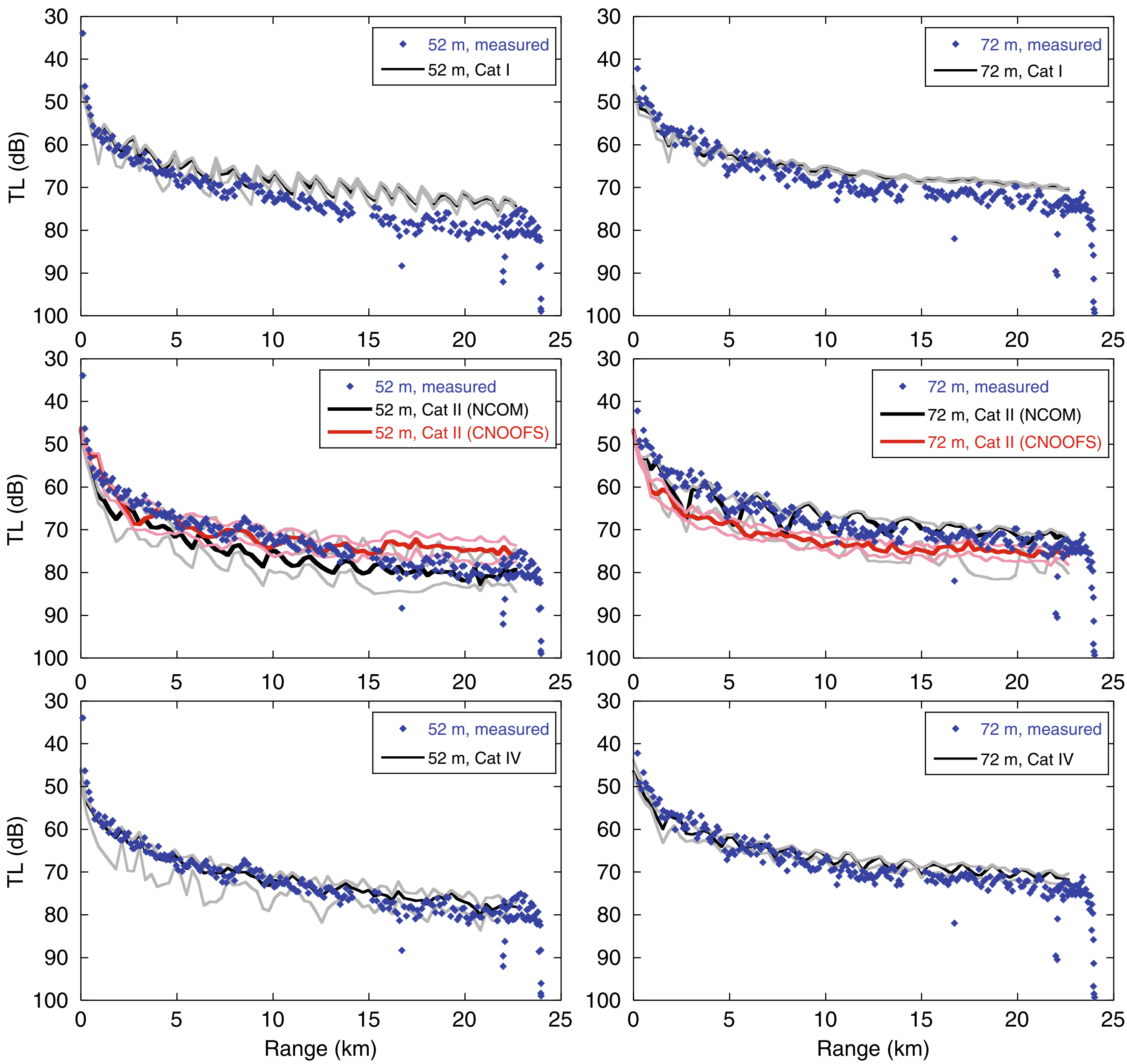

Fig. 12 Comparison of measured transmission loss to model predictions based on categories I, II and IV REA environmental data (*top*, *middle*, *bottom*), for receivers at 52 m (*left*) and 72 m (*right*) depth. *Grey lines* indicate minimum and maximum predicted transmission loss for 1 standard deviation changes in environmental parameters. *Pale red lines* in the *middle* are the same based on C-NOOFS data

the upslope SHARP at 52 and 72 m depths (energy from an 1,100–1,300-Hz LFM) to the modelled mean TL and the expected TL based on the environmental perturbations or uncertainties, that is, the minimum and maximum TL given 1 standard deviation changes in the environmental parameters.

Using category I REA data, TL is underestimated by the model by up to 10 dB at longer ranges for the shallow receiver. In addition, the uncertainties on the loss propagated from the uncertainties on the category I REA data are unrealistically low due to the lack of reasonable uncertainty measurements for the SSP. The

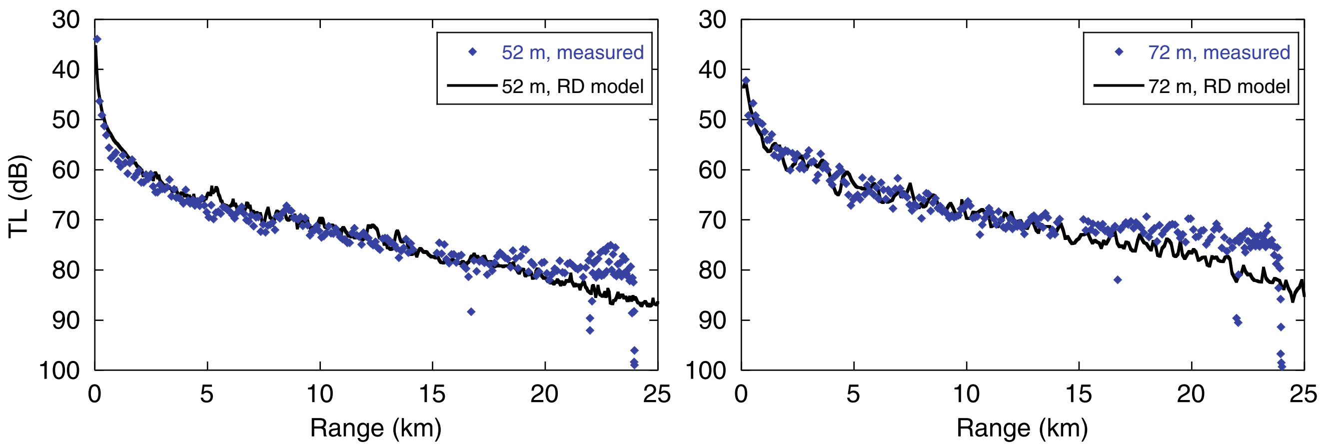

Fig. 13 Comparison of measured transmission loss to model predictions based on category IV REA environmental data using a fully range-dependent model, for receivers at 52 m (*left*) and 72 m (*right*) depth

category II REA gives a more realistic idea of the uncertainty on performance prediction, although the data from the C-NOOFS model in particular overestimates TL for the 72-m receiver, while the NCOM model does likewise for the shallower receiver. The minimum TL prediction for the NCOM model results can lie more than 10 dB below the TL predicted for the mean environmental values, showing the effect of the high-sensitivity region in the middle of the water column that can be seen in Fig. 5. Comparing these results to those found previously, where the category IV sensitivity results using in situ measurements seemed to be in between the two category II results, the measured TL shown in Fig. 12 falls between that found for each model run on the mean parameters. The category IV REA data improve upon the other categories for both receivers. The relatively low spread on possible TL curves for the deeper receiver is due to the lack of sensitivity of the propagation to environmental uncertainty seen in Fig. 8. We can also compare these results to the results found using range-dependent SSP and geoacoustic profiles based on the category IV data (shown in Fig. 13) and in fact the model run on the mean parameters with only range-dependent bathymetry compares well to the model results run with a fully range-dependent 2D model based on the category IV environmental measurements, which overestimates loss at long ranges. Table 4 shows the root mean squared error (RMSE) for the model predictions generated using the sensitivity analysis for each REA category, as well as those for the fully range-dependent model (RD). It is interesting that the error found using the range-dependent model is actually greater than that for the range-independent model using the category IV data. It seems likely that features such as the sound speed minimum, seen at a range of 15 km near 60 m depth in Fig. 6, are representative of phenomena that might exhibit temporal variations that could not be captured during the course of the TL experiment. Focusing and de-focusing effects caused by these would certainly affect the results of the propagation, and without a persistent environmental recording through the length of the experiment might not be incorporated into the model.

An alternative way of displaying the transmission loss and sensitivity information can also be developed that provides a visualization of how the environmental uncertainty impacts performance prediction. Using the 52-m depth analyses, for example, and considering a dipping sonar or towed array, we can calculate the expected, maximum and minimum likely ranges for a given level of signal excess vs. the depth. For example, in Fig. 14, we assume a source at 52 m depth and compute the range at which the TL is less than 70 dB vs. receiver depth. To the right of each plot, the parameter to which the propagation is most sensitive at that range and depth is designated by colour coding.

Table 4 RMSE in decibels for TL predictions

Receiver depth	Category I	Category II (CNOOFS)	Category II (NCOM)	Category IV	RD
52 m	5.07	3.45	3.87	2.16	2.41
72 m	3.34	5.09	3.19	2.82	3.12

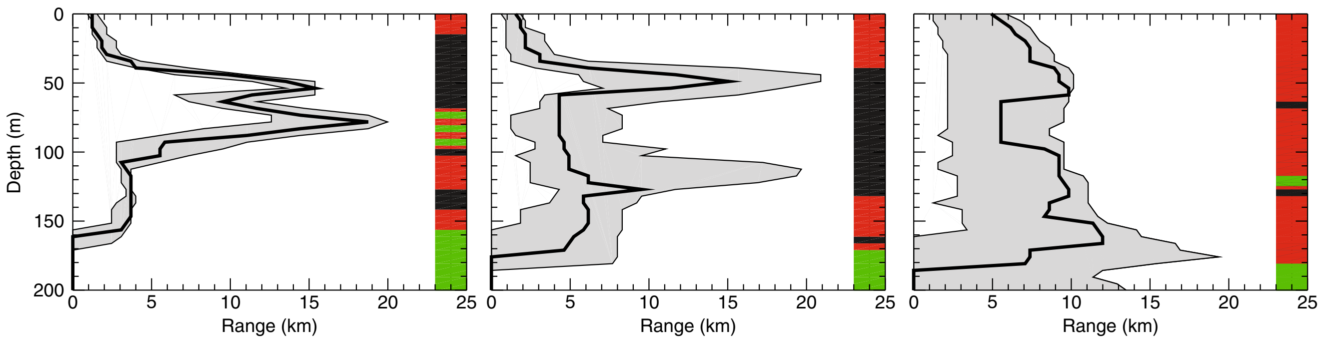

Fig. 14 Expected range for less than 70 dB TL (*black lines*), with minimum and maximum based on environmental uncertainty (*grey*) and dominant sensitivity component vs. depth on the *right side* using colour codes (*red* is c_p, *green* is bathymetry, *dark grey* is SSP). Category II (C-NOOFS) *left*, category II (NCOM) *centre*, category IV (in situ) *right*. Source is at 52 m depth

4 Conclusions

We have presented a set of environmental and acoustic transmission loss data collected during the course of a sea trial and illustrated a simplified method to determine the environmental parameters to which acoustic propagation is most sensitive in a given environment as a function of source and receiver geometry using a prototype tactical decision aid, the PASTET. Unsurprisingly, the important parameters and measurements required depend on environment, range and depth. The results from the linearized sensitivity measure incorporated in PASTET were compared to the sensitivities obtained using a non-linear Monte Carlo sensitivity calculation. Although for the most part the linearized sensitivity measure gives both the same range–depth pattern as the non-linear measure and identifies the parameters to which propagation is most sensitive, it tends to underestimate the sensitivity, which differs from previous results found using these measures (Dosso et al. 2007). The linearized sensitivity measure can certainly be of use, especially in situations where real-time results are required, an initial comparison through the earlier stages of acquisition of REA data to the non-linear measure is important.

A set of transmission loss model runs using REA data were also performed using PASTET, which also generated an envelope of expected TL based on the environmental uncertainty. In general, a progression through the categories of REA data resulted in an improved model–data agreement. A good estimate of propagation uncertainty depends on having a reasonable initial estimate of environmental uncertainty, which may not be available in the earliest categories of REA. However, the question of what is sufficient is still one that must be driven by operational requirements.

Acknowledgements We would like to acknowledge the contributions of MetOc Halifax, the Department of Fisheries and Oceans—Northwest Atlantic Fisheries Centre (NAFC), Naval Research Laboratory Stennis, Dalhousie University—Department of Oceanography and colleagues at DRDC Atlantic.

References

Antonov J, Locarnini R, Boyer T, Mishonov A, Garcia H (2006) World Ocean Atlas 2005, vol 2, salinity. In: Levitus S (ed) NOAA atlas NESDIS, vol 62. NOAA, Silver Spring, p 182

Bershad S, Weiss M (1975) Deck 41 surficial sediment database. NOAA National Geophysical Data Center, Boulder

Chen C, Millero F (1977) Speed of sound in seawater at high pressures. J Acoust Soc Am 62(5):1129–1135

Del Grosso V (1970) Sound speed in pure water and sea water. J Acoust Soc Am 47(3):947–949

Dosso S, Giles P, Brooke G, McCammon D, Pecknold S, Hines P (2007) Linear and nonlinear methods of ocean acoustic environmental sensitivity. J Acoust Soc Am 121(1):42–45

Dosso S, Morley M, Giles P, Brooke G, McCammon D, Pecknold S, Hines P (2007) Spatial field shifts in ocean acoustic environmental sensitivity analysis. J Acoust Soc Am 122(5):2560

Finette S (2006) A stochastic representation of environmental uncertainty and its coupling to acoustic wave propagation in ocean waveguides. J Acoust Soc Am 120(5):2567–2579

Flatté S, Dashen R, Munk W, Watson K, Zachariasen F (1979) Sound transmission through a fluctuating ocean. Cambridge University Press, Cambridge

Furlong M, Kostylev VE, Orpin AR (2006) Bathymetry-based model for reconstruction of seabed texture on the Scotian-Fundy continental margin. In: Proceedings of Canadian hydrographic conference, Halifax, NS, 5–9 June 2006

Giles PM, Kilistoff S, Brooke G (2009) Portable acoustic sensitivity and transmission evaluation tool–PASTET. Contract Report CR2008-209, Defence R&D Canada—Atlantic

Jackson D (1994)APL-UW high-frequency ocean environmental acoustic models handbook. Technical report 9407, Applied Physics Laboratory, University of Washington

Krolik JL (1992) Matched-field minimum variance beamforming in a random ocean channel. J Acoust Soc Am 92(3):1408–1419

LeBlanc LR, Middleton FH (2006) An underwater acoustic sound velocity data model. J Acoust Soc Am 67(6):2055–2062

LePage K (2006) Modeling propagation and reverberation sensitivity to oceanographic and seabed variability. IEEE J Oceanic Eng 31(2):402–412

Locarnini R, Mishonov A, Antonov J, Boyer T, Garcia H, Levitus S (2006) World Ocean Atlas 2005. In: Levitus S (ed) Temperature, vol 1. NOAA atlas NESDIS, vol 61. NOAA, Silver Spring, p 182

Madec G (2006) NEMO ocean engine. Note du Pôle de Modélisation, Institut Pierre-Simon Laplace

McCammon D, Dosso S, Morley M, Giles P, Brooke, G (2007) The sensitivity of transmission loss modeling to environmental resolution: Emerald Basin bathymetry and sediment composition. Tech. rep. CR 2007-103, DRDC Atlantic

National Geophysical Data Center (2011) ETOPO2v2 Global Gridded 2-minute Database. National Geophysical Data Center, National Oceanic and Atmospheric Administration, U.S. Dept. of Commerce, Boulder

Osler J, Furlong A, Christian H (2006) A sediment probe for the rapid assessment of seabed characteristics. In: Acoustic sensing techniques for the shallow water environment, pp 171–181

Pace NG, Jensen FB (eds) (2002) Impact of littoral environmental variability on acoustic predictions and sonar performance. Kluwer Academic, Dordrecht

Porter M, Bucker H (1987) Gaussian beam tracing for computing ocean acoustic fields. J Acoust Soc Am 82(4):1349–1359

Potter J, Warn-Varnas A (eds) (1990) Ocean variability and acoustic propagation. Kluwer Academic, Dordrecht

Rhodes R, Hurlburt H, Wallcraft A, Barron C, Martin P, Smedstad O, Cross S, Metzger E, Shriver J, Kara A et al (2002) Navy real-time global modeling systems. Oceanography 15(1):29–43

Robertson P (1991) Soil classification using the cone penetration test: Reply. Can Geotech J 28(1):176–178

Rouseff D, Ewart TE (1995) Effect of random sea surface and bottom roughness on propagation in shallow water. J Acoust Soc Am 98(6):3397–3404

Thorsos EI, Henyey FS, Williams KL, Elam WT, Reynolds SA (2002) Simulations of temporal and spatial variability in shallow water propagation. In: Pace NG, Jensen FB (eds) Impact of littoral environmental variability on acoustic predictions and sonar performance. Kluwer Academic, Dordrecht, pp 337–344

Whitehouse B, Vachon P, Thomas A, Quinn R, Renaud W (2006) Rapid environmental assessment (REA) of the maritime battlespace. Can Mil J 66–68

Wong G, Zhu S (1995) Speed of sound in seawater as a function of salinity, temperature, and pressure. J Acoust Soc Am 97(3):1732–1736